Research Work

Title: Understanding the regulatory role of PAD-4 on Del-1 and evaluation of PAD-4 inhibitors in pulmonary fibrosis

1. Introduction

Citrullination is a major post-translation modification (PTM) which is mediated by the enzyme peptidyl arginine deiminase (PAD). It catalyses the deimination reaction of peptidyl arginine moiety and thereby converting it into citrulline that is a non-protein amino acid. There are five PADs present namely PAD-1, PAD-2, PAD-3, PAD-4 and PAD-6 with calcium as a major co-factor for their activation (1). These enzymes have tissue specific localisation and takes part in various physiological processes, thus maintaining homeostasis. For instance, PAD-1 is expressed in uterus and epidermis, PAD-2 is expressed in skeletal muscles, brain and immune cells, PAD-3 is expressed in hair follicles and skin, PAD-4 expressed in neutrophils, macrophages, granulocytes, inflammatory cells and neoplastic cells and PAD-6 is expressed in oocytes and embryos (1). PAD-4 is present in immune cells such as neutrophils, macrophages, granulocytes, monocytes, natural killer cells and cancer cells .This enzyme has the ability to migrate to the nucleus and induce citrullination of the nuclear histone proteins such as H2A, H3 and H4. However, among all the PAD enzymes found in humans, only PAD-4 and recently PAD-2 are known to migrate to nucleus and catalyse citrullination of histones by converting arginine to citrulline on the histone H3 of chromatin structure (1,2). By the virtue of modifying peptidyl arginine of histone moieties, PAD-4 mediates the formation of neutrophil extracellular traps (NETs) in neutrophils. The process of formation of NETs known as NETosis is a major mechanism of anti-microbial defence by neutrophils other than phagocytosis. These NETs are the mesh like structures consisting of decondensed chromatins, neutrophil elastase (NE) and cathepsin G that are a group of serine proteases, myeloperoxidase (MPO) that is a peroxidase, matrix metalloproteinase (MMPs), tissue inhibitors of MMPs (TIMPs) and abundant amount of ROS. PAD-4 migrates to the nucleus, modifies histone arginine to citrulline, reducing histone positivity and disrupting chromatin and histone bonding thereby leading to chromatin decondensation and release in the form of NETs (1,2). Exaggerated NETs release mediated by dysregulation of PAD-4 activity, production of ROS and severe inflammation which then induces a vicious cycle of inflammation accompanied by repetitively stimulation of other cells of fibroblasts leading to higher production of pro-inflammatory and pro-fibrotic cytokines results in PF progression (Figure 1) (3).

Pulmonary fibrosis (PF) results from recurring injury to the lungs leading to extensive inflammation during the initial inflammatory phase and dysregulated wound healing response during the late fibrotic phase that results in the epithelial-mesenchymal transition (EMT) and development of excessive connective tissue and increase in deposition of the extracellular matrix (ECM) components (4–7). Under normal condition, inflammatory cells are activated during an external or internal injury where they tend to clear out the antigen and secrete cytokines like tumor necrosis factor- α (TNF-α), interleukins and transforming growth factor-β1 (TGF-β1) that stimulate fibroblasts. These fibroblasts differentiate into myofibroblasts that secrete proteins of ECM to close the wound healing process (8). This is succeeded by clearing of the activated myofibroblasts by which the wound healing process is closed. However, the recurring insults of PF results in alveolar epithelial cell damage, resulting in a sustained inflammation and prolonged fibrotic response with dysregulated EMT and significant deposition of the ECM proteins that significantly alters the lung architecture and function. The fibroblasts and myofibroblasts are in continuous exposure to cytokines and growth factors such

as TGF-β1, platelet derived growth factor (PDGF) and connective tissue growth factor (CTGF) leading to their exaggerated activation (4,5,9–11).

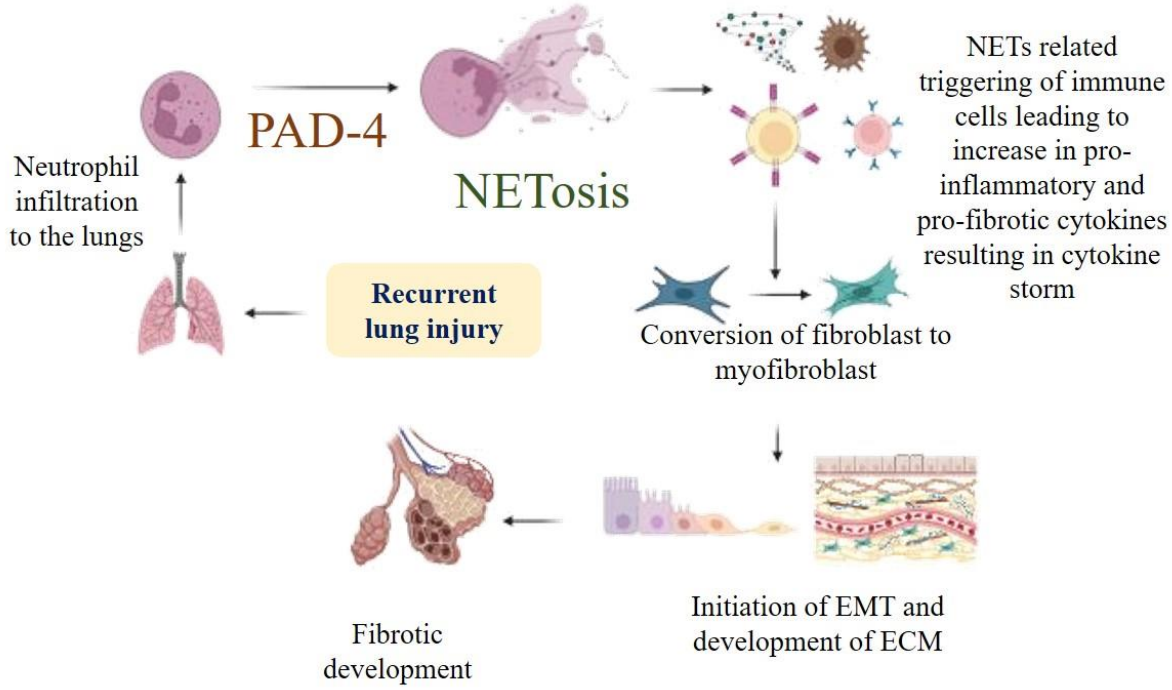

Figure 1: The role of PAD-4 mediated NETosis in the progression of PF.

The investigation into the protective role of various anti-inflammatory factors and mediators has revealed developmental endothelial locus-1 (Del-1) as one such mediator, primarily expressed by endothelial cells in lungs and neural cells in brain (12,13). It is also known as epidermal growth factor (EGF)-like repeats and discoidin I-like domains 3 (EDIL3). This protein, homologous to milk fat globule epidermal growth factor-8 (MFG-E8) can restrict leukocyte recruitment by inhibiting the interaction of leukocyte function antigen (LFA) to its receptors, such as intercellular adhesion molecule-1 (ICAM-1) on immune cells' surfaces. Del-1 is also involved in regulating ECM formation and composition. Del-1 inhibits TGF-β1 activation and also possess anti-fibrotic properties (13). Furthermore, Del-1 enhances efferocytosis, phagocytosis of apoptotic cells by macrophages, by bridging the gap between apoptotic cells and macrophages. Additionally, Del-1 inhibits the nuclear factor kappa B (Nf-κB) pathway, indirectly suppressing multiple pro-inflammatory pathways (14,15). PAD-4 has been reported to interact with and repress the p53 gene, a tumor suppressor and regulator of various signalling pathways, which in turn regulates multiple p53 target genes, including Del-1(16). The presence of multiple p53 response elements in the promoter region of the Del-1 gene suggests a direct upregulation of Del-1 transcription by p53, with inhibition of p53 leading to reduced Del-1 expression in murine primary endothelial cells, indicating a potential interaction between PAD-4 and Del-1 through p53 gene (17).

In the early stage a pre-existing antitumour/antibiotic aminoquinone derivative streptonigrin was identified as PAD-4 inhibitor with IC50 value of 1.87 ± 0.24 μM among the library of >2000 compound. The kinetics study among PADs isoenzymes revealed a significant selectivity for PAD-4 (18–20).Thereafter, 2-chloroacetamidine was found to display the activity against PAD-4 (IC50 ≈ 500 μM).7 Subsequently, benzoyl-L-arginine amide (BAA)

was identified as decent binding substrate for PAD-4. The F- and Cl-amidine (CLA) warhead installed frameworks were evaluated against PADs, in which CLA exhibited comparatively higher potency in PADs 1-4 (21–23). The unnatural D-isomers 4c-d were highly selective (200 - 400 folds) towards PAD-1, which might be attributed to better metabolic stability (24). Later, the introduction of ortho-COOH functionality led to the more potent derivative o-F-amidine and o-CLA for F- and CLA, respectively (25). The peptidic nature of these first-generation inhibitors possessed various limitations, including reduced metabolic stability and poor membrane permeability. This led to the development of second-generation inhibitors by introducing further modification in lipophilic carboxamide backbone. Alteration of C-terminal carboxamide to benzimidazole and N-terminal phenyl with biphenyls resulted BB-F/Cl-amidine (25–28). The increased lipophilicity of 6a-b led to improved cell permeability, perhaps the in vitro efficacy remains unaltered. A further modification to introduce substituted benzimidazole along with the N-terminal lactams resulted in another set of molecules, which were found to be more selective towards PAD-2 (≈100 fold) (28). Later modification to C-terminal benzylamide and N-terminal naphthalene moiety, produced improved inhibition of cellular proliferation due to higher lipophilicity/cell permeability.37 However, the finding a significant selectivity among PAD isoforms is still a demanding area of research.

2. Hypothesis

The PAD-4 enzyme is of utmost necessity for the initiation of NETosis and anti-microbial defence. However, exaggeration of NETosis is implicated in development of PF. PAD-4 is also involved in the repression of anti-inflammatory molecule Del-1 which is a p53 target gene. Our first hypothesis involves evaluation of the standard PAD-4 inhibitor i.e. chloro-amidine (CLA) in the *in vivo* model of bleomycin (BLM) induced PF. We will also evaluate the role of CLA on the mRNA and protein levels of Del-1. Macrophages and neutrophils go hand in hand in exhibiting inflammatory response. We will evaluate the effects of inhibition of PAD-4 mediated NETs on the M1/M2 macrophage polarisation. We will evaluate the time-dependent inhibition of PF by CLA and the effects CLA has on the M1 macrophage during early inflammatory phase and on the M2 macrophage during the late fibrotic phase. We will also be developing novel chemical entities (NCEs) against PAD-4 that are thought to resist fibrotic changes by decreasing the extent of inflammation and fibrosis.

3. Objectives

- To understand the regulatory effect of PAD-4 on Del-1 in pulmonary fibrosis models
- To screen the novel PAD-4 inhibitors and optimize the compounds through *in vitro* studies
- Evaluation of *in vivo* anti-fibrotic effects of the most potent PAD-4 inhibitor and study its fibrosis resolving effects

4. Materials and methods

4.1 Materials required

BLM was purchased from Celon labs (India). JC-1 dye, CLA, 5, 5-dithio-bis(2-nitrobenzoic acid) (DTNB), bovine serum albumin (BSA), phorbol 12-myristate 13-acetate (PMA) were purchased from Sigma-Aldrich (USA). Most of the other chemicals used for biochemical assays including bradford reagent, sodium dodecyl sulphate (SDS) , 2-thiobarbituric acid (TBA), tetra-methoxy propane (TMP), radioimmunoprecipitation assay (RIPA) lysis buffer, 4′,6-diamidino-2-phenylindole (DAPI), 2',7'-dichlorofluorescin-diacetate (DSCFDA) were purchased from Sigma-Aldrich (USA). MitoSOX red reagent, Sytox green dye, lysotracker red dye and enzyme-linked immunosorbent assay kits were purchased from Invitrogen (USA). Cell culture media including Roswell Park Memorial Institute (RPMI) and minimum essential media (MEM) were purchased from Cytiva (USA). PAD-4 inhibitor screening assay kit was purchased from Cayman chemical (USA). Chemicals necessary for staining techniques like direct red, picric acid, toluidine blue, and haematoxylin and eosin solutions were also obtained from Sigma-Aldrich (USA). Fluorescently labelled F4/80 antibody was purchased from Cell Signalling Technologies (USA). Antibodies including primary antibody secondary raised against mouse, goat and rabbit and fluorescently labelled secondary antibodies were purchased from Santa Cruz Biotechnology (USA) unless stated otherwise. Primary antibody against Ly6G was purchased from Biolegend (USA). Primary antibody against NE and CitH3 were purchased from Novus biologicals (USA). Primary antibody against MPO was purchased from cell signalling technologies (USA). Primers for real time-polymerase chain reaction (RT-PCR) for PAD-4 and Del-1 were purchased from GCC Biotech (India) whereas primers for α-SMA and TGF-β1, p53 and Col1A1 were purchased from Integrated DNA Technologies (USA). All other primers were purchased from Eurofins Genomics (France). The new chemical entities were synthesised in collaboration with the medicinal chemistry department of NIPER Hyderabad.

4.2 Methods

The *in vitro* anti-NETotic assays were carried out in differentiated HL-60(dHL-60) cells. The HL-60, pro-myeloblastic leukemic cells that gain the phenotype of neutrophils upon differentiation with 70mM dimethylformamide (DMF). The dHL-60 cells were plated and induced NETosis with phrobol 12-myristate 13-acetate (standard inducer(PMA)) at 500nM concentration followed by treatment with CLA at 100µM concentration for 4 hours followed by addition of sytox green dye (200nM), a live cell impermeable DNA staining dye that stains extracellular DNA and an excellent detector of NETs release. This was followed by evaluation of oxidative stress through DCFDA, nitrite through Griess assay, MPO and immunocytochemistry (ICC) analysis as mentioned in the previously described protocol (2). The dHL-60 cells were stimulated with 500nM of PMA and treated with 100µM of CLA following which NETs were isolated based on an earlier report (29). The THP-1 monocytes were exposed to the isolated NETs at 1000ng/ml concentrations. DCFDA, MitoSOX, and ICC analysis were carried out to evaluate oxidative stress, NETotic and fibrotic markers(2,30,31). Synthesised NCEs were subjected to kit based PAD-4 enzyme inhibition carried out as per manufacturer's instructions (Item no. 700560, Cayman chemicals, USA). This was followed by evaluation of cytotoxicity and NETosis in the dHL-60 cells using MTT and Sytox green (200nM) assay following the treatment duration. Oxidative stress and nitrite levels using DCFDA and Griess assay. NETs were isolated from PMA stimulated and NCE treated dHL-60 cells based on the previous mentioned report and exposed to MRC-5 fibroblasts(29).

Following exposure, cellular and mitochondrial oxidative stress was evaluated in the fibroblasts. Fibrotic markers were evaluated through biochemical assays, ICC, RT-PCR and western blotting(2,30,31).

For animal studies following completion of treatment duration, the animals were subjected to whole body plethysmography (WBP) before sacrifice. Then the animals were euthanised and following euthanisation, bronchoalveolar lavage fluid (BALF) and blood were isolated and evaluated for fibrotic and inflammatory parameters. Biochemical tests for evaluation of levels of nitrite, GSH, MDA, hydroxyproline and MPO were carried out as per previous mentioned protocols (2,6,7,32,33). Evaluation of the levels of pro-inflammatory and pro-fibrotic cytokines were carried out as per manufacturer's instructions through ELISA (catalogue no. 88-7346-88, 88-7066-22, 88-7261-22 and 88-50390-22, Invitrogen, USA). The formalin fixed tissues were subjected to Haematoxylin and Eosin (H&E), picrosirius red (PSR) and masson's trichrome (MT) analysis as per the previous mentioned protocols (2,6,7,32,33). Further, immunohistochemistry (IHC), immunofluorescence (IF), RT-PCR and western blotting (WB) were also carried out as per our laboratory standardised methods (2,6,7,32,33).

5. Results

5.1 To understand the regulatory effect of PAD-4 on Del-1 in pulmonary fibrosis models

5.1.1 Experimental Design

The cells were divided into three groups with one normal control, one group received PMA and other group received PMA with CLA. Following treatment for 4 hours, the cells were harvested and evaluated for NETotic markers.

The animals were divided into five groups following randomisation where the groups except normal control received BLM at 1.5 U/kg on day 0 through oro-pharyngal instillation. The low dose treatment group received 3 mg/kg of CLA and the high dose treatment group received 10 mg/kg of CLA which was administered intra-peritoneally (IP). The final treatment group received the standard anti-fibrotic drug PFD at 200 mg/kg dose through oral route. The treatment was continued for a period of 28 days.

5.1.2 Results

We first evaluated the anti-NETotic effects of CLA in differentiated HL-60 (dHL-60) cells. CLA (100µM) showed reduced levels of nitrite and DCFDA fluorescence reflecting reduced levels of inflammation. It also showed decreased relative fluorescence of sytox green stain corroborated with decreased NETs, MPO levels and reduced cellular expression of PAD-4 compared to NETs stimulation with PMA (Figure 2). Evaluation of lung functional parameters through WBP showed CLA effectively ameliorated the lung functional parameters dose-dependently which is accompanied by restoration of body weight, lung weight and lung appearance in comparison to BLM induced fibrotic lungs (Figure 3A). BALF fluid isolation revealed decreased total cell count in BALF with reduced levels of albumin and total protein compared to BLM induced fibrotic lungs (Figure 3B). Upon isolation of blood neutrophils, it was found that CLA treated group showed decreased count of total neutrophils with reduced NETotic potential (Figure 3C). The histopathological analysis revealed clear depiction of alveolar septa, reduced inflammatory infiltration and oedema in comparison to BLM induced

fibrotic lungs. Moreover, histopathological studies also reflected decreased collagen deposition in the lung tissues (Figure 3D). Oxidative stress evaluated through biochemical evaluation demonstrated that CLA reduced the levels of nitrite and MDA and increased the levels of anti-oxidant GSH (Figure 3E). Furthermore, the CLA treated animals showed decreased levels of pro-inflammatory cytokines like TNF-α, IL-6 and IL-1β and pro-fibrotic cytokine TGF-β1 compared to BLM induced fibrotic lungs. The decrease in collagen content in the lung tissues is accompanied with decreased deposition of proteins of extracellular matrix like collagen 1A1 and fibronectin (Figure 3F-H). We also showed that CLA reduced the expression of mesenchymal markers α-SMA and N-cadherin, transcription factor potentiating EMT like SNAIL and SLUG and markers for matrix remodelling and fibrogenesis compared to BLM induced fibrotic lungs (Figure 3I-M). Moreover, CLA being a PAD-4 inhibitor, decreased the expression of NETotic markers like PAD-4, NE, MPO and CitH3 and increased the levels of p53 and Del-1. Thus, it was confirmed that PAD-4 inhibition significantly ameliorated PF and this amelioration was also supported by increase in anti-inflammatory anti-fibrotic mediator Del-1levels (Figure 3M-S). This work is published in International Immunopharmacology journal having an impact factor of 4.8.

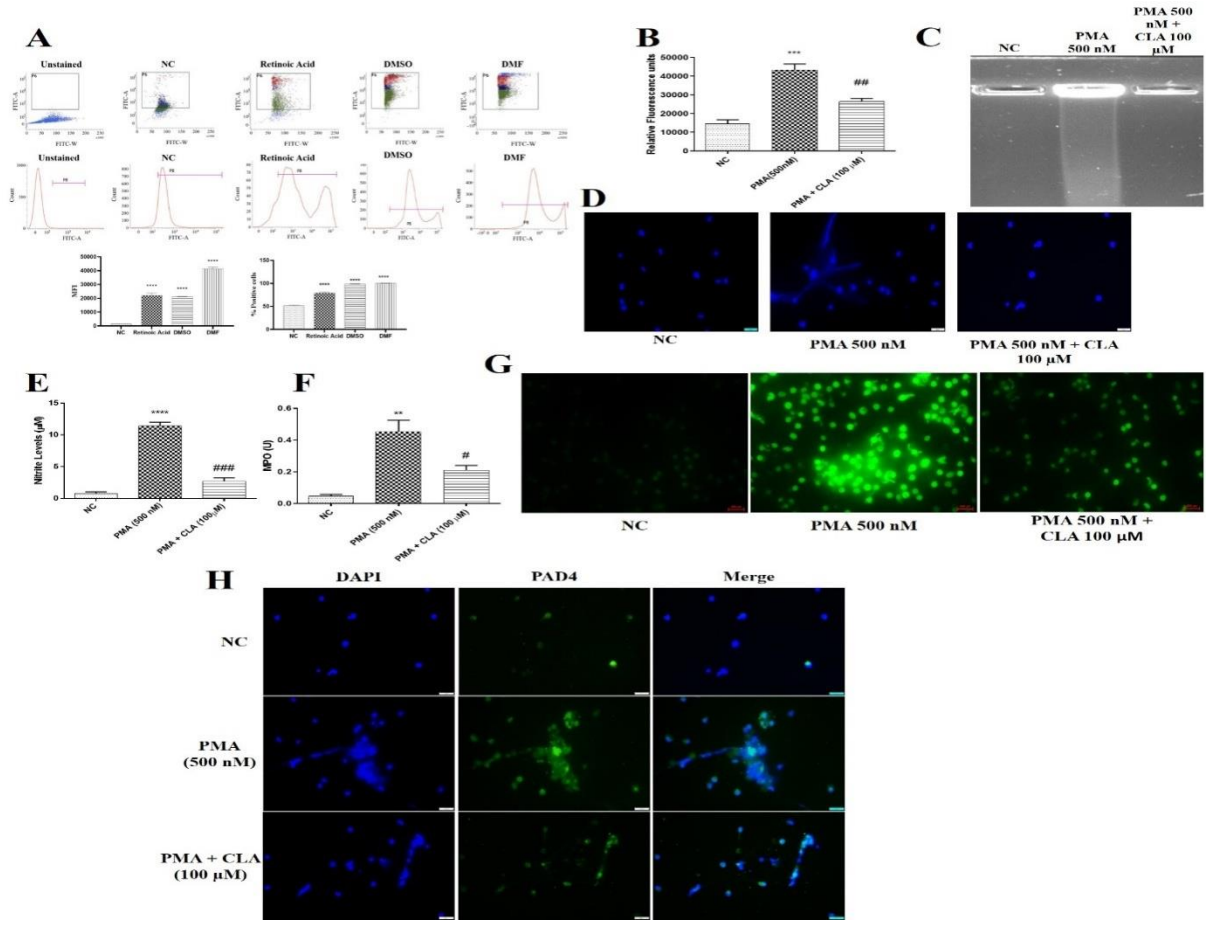

Figure 2: Effects of CLA on NETosis and inflammation *in-vitro* in dHL-60 cells. A) Flow cytometric analysis of the effect of differentiating agents on HL-60 cells, B) Quantification of sytox relative fluorescence units of dHL-60 cells, C) Agarose band depicting NETs, D) DAPI staining, E and F) Nitrite and MPO levels, G) DCFDA staining and H) PAD-4 expression. All results are expressed as mean±SEM of n=3. **p<0.01, ***p<0.001 and ****p<0.0001 vs NC, #p<0.05, ##p<0.01 and ###p<0.001 vs PMA.

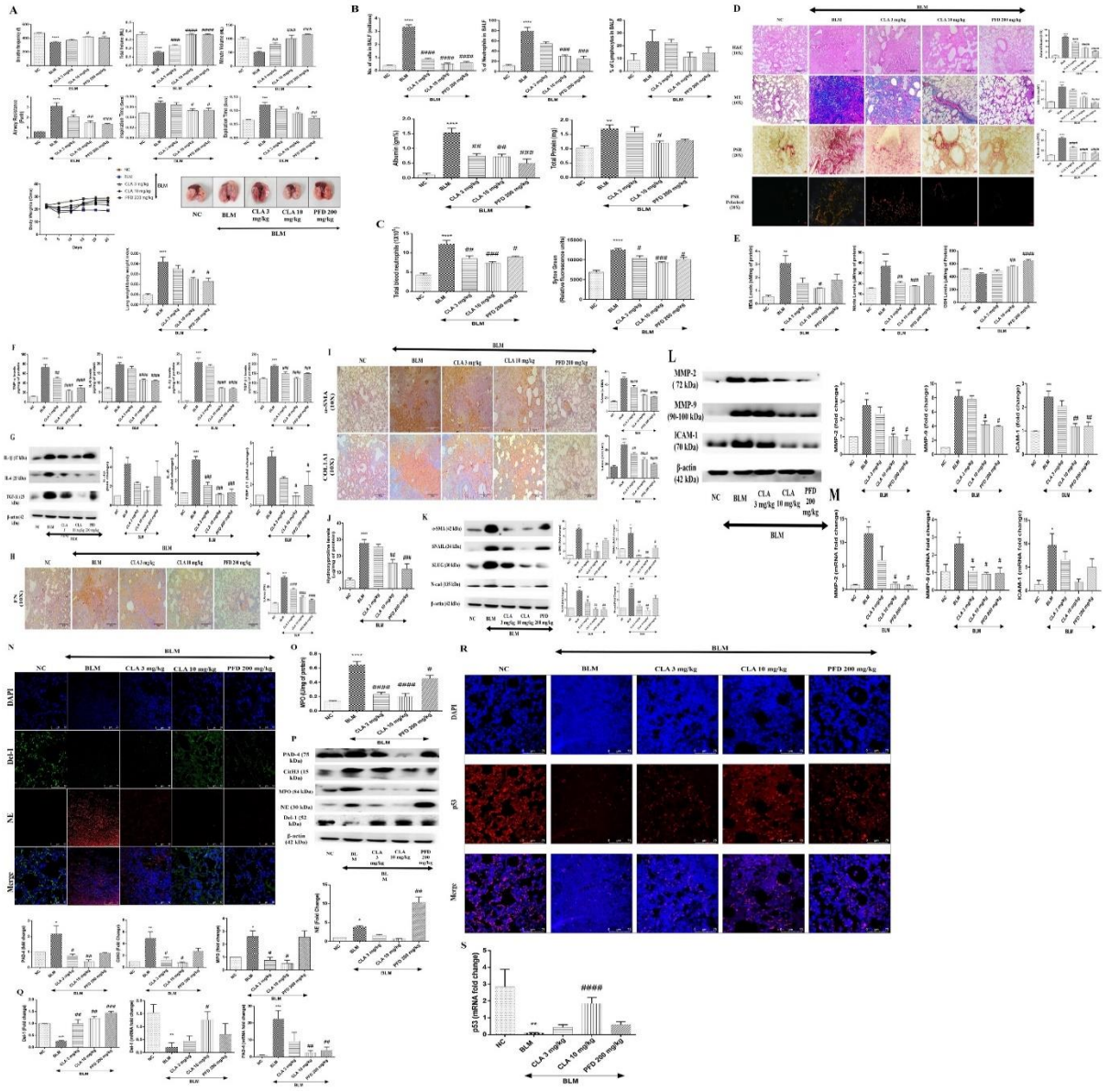

Figure 3: Effect of PAD-4 inhibitor CLA on A) Lung functional parameters, body weight, lung weight(n=8), B) BALF parameters(n=4), C) Neutrophilic parameters(n=4), D) H&E, PSR and MT stainings and their quantification(n=3), E) Biochemical oxidative stress(n=8), F-K) Inflammatory and fibrotic markers quantified by IHC(n=10) ELISA(n=8) and WB(n=3), L, M) Markers for matrix remodelling and fibrogenesis quantified by WB(n=3) and RT-PCR(n=4), N-S) NETotic markers, expression of Del-1 an p53 quantified by biochemical assay(n=8), WB(n=3) and RT-PCR(n=4). H&E images were taken at 10X, PSR, MT and IHC images at 20X and the confocal images at 40X magnification. All results are expressed as mean±SEM of.*p<0.05, **p<0.01, ***p<0.001 and ****p<0.0001 vs NC, #p<0.05, ##p<0.01, ###p<0.001 and ####p<0.0001 vs BLM.

5.2 To screen the novel PAD-4 inhibitors and optimize the compounds through *in vitro* studies

5.2.1 Experimental Design

The dHL-60 cells were divided into seven groups with one normal control, one PMA control, four NCE treatment groups and one standard CLA treatment group. PMA was stimulated to induce NETs in all groups except normal control. The treatment groups received respective NCEs at their IC_{50} concentrations. Following treatment of 4 hours, cells were harvested and assay for identification of NETotic parameters were carried out.

The fibroblasts were divided into 6 groups with one normal control, one group received NETs isolated from PMA stimulated dHL-60 cells and other groups received NETs isolated from PMA stimulated and NCE treated dHL-60 cells. Upon completion of 24 hour exposure duration, the cells were harvested and evaluated from fibrotic markers.

5.2.2 Result

In the earlier two studies it was confirmed that PAD-4 inhibition ameliorated NETosis, inflammation and fibrosis in mice models of BLM induced PF. Here, we have synthesised NCEs against PAD-4 and evaluated anti-NETotic and anti-fibrotic effects in *in vitro* and *in vivo* models of PF. NCEs were synthesised based on the available PAD-4 inhibitors from literature. A total of 202 experimentally designed molecules were subjected to molecular docking analysis using Schrödinger Suite 2020-3. After detailed analysis of molecular docking results, focus shifted towards synthesizing selected molecules; where the primary aim was to synthesize indole-pyrazolopyrimidine derivatives. The synthesis of indole-pyrazolopyrimidine derivatives was carried as per known procedures which included three key intermediates i.e. indole-pyrazole amines α,β-unsaturated carbonyls and benzylidenes. The synthesis begin with *N*-alkylation of indole moieties with alkyl iodides in presence of sodium hydride in DMF to procure N-alkylated indoles. Then, the indoles were treated with cyanoacetic acid in acetic anhydride to obtain β-ketonitriles. Next, the β-ketonitriles were reacted with NH_2-$NH_2 \cdot H_2O$ in the presence of catalytic amount of methane sulfonic acid under reflux to access pyrazole amines. Other key intermediates i.e. α,β-unsaturated carbonyls was synthesized by reacting various acetophenones with DMF-DMA under reflux. On other side, different benzaldehydes were reacted with malononitrile in presence of DBU in THF at room temperature to obtain benzylidenes. Finally, pyrazole amines were treated with α,β-unsaturated carbonyl compounds under reflux in acetic acid or with benzylidenes in ethanol:pyridine (2:1) under microwave irradiation to produce the desired products indole-pyrazolopyrimidine derivatives 35a-i and 36a-n, respectively. The individual chemical structure and yield of prepared series of molecules is presented below in Figure 4A. The 23 synthesised molecules then were subjected to evaluation of anti-NETotic effects in dHL-60 cells and anti-fibrotic effects in MRC-5 fibroblasts. Firstly, the NCEs were evaluated for their cytotoxicity and NETs inhibitory potential in dHL-60 cells. It was followed by PAD-4 enzyme specific inhibition through kit based method (Figure 4B). Based on the obtained results for cytotoxicity, percentage of NETs inhibition and PAD-4 enzyme inhibition results, 4 compounds namely 35a, 36a, 36e and 36j showed significant effects in comparison to other molecules and hence, these four molecules were selected for further anti-NETotic and anti-fibrotic effects *in vitro*. These molecules significantly inhibited oxidative stress which was increased upon PMA stimulation in dHL-60 as evident from decreased nitrite and decreased DCFDA fluorescence intensity (Figure 5A). Further, extended NETotic evaluation suggested significant inhibition of sytox green staining

as evident from flow cytometry and fluorescence images with 36e molecule showing significantly higher effects than other NCEs (Figure 5B, C). This is also corroborated by decreased expression of NETotic markers such as CitH3, MPO, NE and PAD-4 in the NCE treated dHL-60 cells compared to PMA stimulated cells (Figure 8D-M). The anti-fibrotic evaluation of these NCEs were carried out using the NETs isolated from specific treatment groups. NETs were isolated from previously described protocol and then the MRC-5 fibroblasts were exposed to 1000 ng/ml of isolated NETs. The MRC-5 fibroblasts exposed to NCE treated NETs showed decreased levels of cellular and mitochondrial oxidative stress compared to fibroblasts exposed to PMA stimulated NETs (Figure 6A, B). Migration is an inherent property of fibroblasts and the activated fibroblasts shows greater degree of migration. The MRC-5 cells exposed to NCE treated NETs showed decreased migratory potential in comparison to fibroblasts exposed to PMA stimulated NETs with the molecule 36e showing better activity than other molecules (Figure 6C). Further, we evaluated the expression of markers for mesenchymal cells, EMT and fibrogenesis. We observed higher expression of fibrotic markers such as α-SMA, vimentin, TGF- β1, FGF-15, ICAM-1 and COL1A1 in the fibroblasts exposed to PMA stimulated NETs. However, the fibroblasts exposed to NCE treated NETs showed decreased levels of these markers with the molecule 36e showing significant effects than other molecules (Figure 6D-O). Based on the results of PAD-4 inhibition and anti-NETotic and anti-fibrotic studies, 36e molecule was selected for detailed *in vivo* evaluation of anti-fibrotic effects in BLM induced PF animals.

A

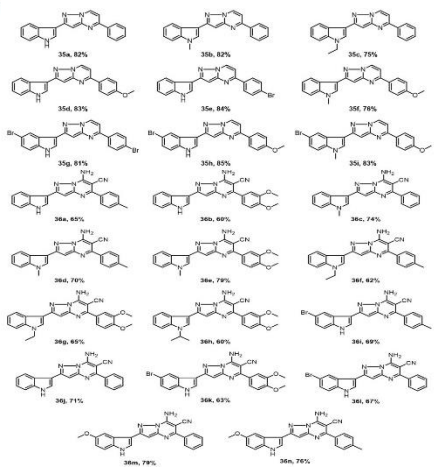

B

Compounds	Docking Score	IC50 of enzyme inhibition through kit based method (μM)	IC50 of cell viability (μM)	Percentage of NETs inhibition through sytox green
35a	-5.30793339	14.37±2.31	12.57±1.68	80.02±0.59
35b	-4.626111799	No inhibition	6.34±2.15	61.47±6.88
35c	-4.314513495	No inhibition	9.04±5.25	51.46±2.38
35d	-4.265430113	No inhibition	5.09±1.12	46.44±7.53
35e	-4.966905348	19.21±9.21	4.20±0.43	30.66±0.21
35f	-5.118183907	No inhibition	4.29±1.03	60.07±3.96
35g	-5.412106474	No inhibition	3.57±0.09	57.67±2.01
35h	-4.475731718	25.36±14.27	7.11±1.72	33.11±0.85
35i	-4.968113972	No inhibition	6.18±0.62	57.11±1.60
36a	-5.826146321	9.66±0.67	15.81±1.84	78.45±2.12
36b	-5.916955338	11.28±1.56	4.71±0.70	58.32±1.91
36c	-5.597116588	13.1±0.68	4.21±0.42	69.48±1.34
36d	-5.47365276	12.14±3.33	7.02±2.40	43.29±7.57
36e	-6.207321862	5.64±0.30	14.69±1.53	84.34±1.52
36f	-5.37002132	9.92±4.37	4.53±0.17	53.97±0.86
36g	-5.947818863	12.85±6.79	3.17±0.19	58.87±2.45
36h	-4.915917696	No inhibition	5.29±0.60	48.42±8.17
36i	-5.700478823	9.31±2.41	2.92±0.14	73.14±0.43
36j	-4.843040791	7.83±1.54	21.21±1.42	74.04±1.64
36k	-5.760903008	4.54±0.76	6.82±1.61	29.53±2.37
36l	-5.81774434	4.74±0.76	2.68±0.32	37.92±5.09
36m	-5.947579038	4.98±0.52	2.13±0.08	46.84±3.09
36n	-5.50718571	5.77±1.97	2.47±0.16	74.84±0.51
CLA	-6.803	6.08±0.58	9.05±1.07	81.44±1.25

Figure 4: A) Synthesized indole pyrazolopyrimidine derivatives (35a-i and 36a-n) and B) Docking score, PAD-4 enzyme inhibition, cytotoxicity and percentage of NETs inhibition of the NCEs.

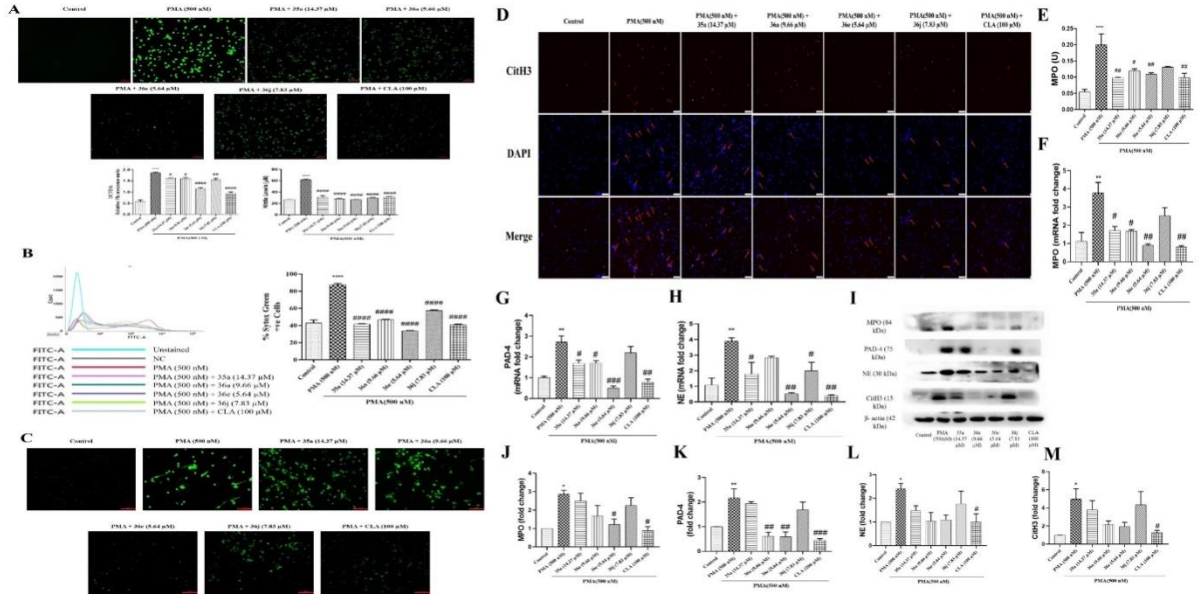

Figure 5: Effect of selected NCEs (35a, 36a, 36e and 36j) on A) oxidative stress indicated by DCFDA and Nitrite levels, B, C) Flow cytometric analysis and fluorescent images of sytox green positive cells, D) Expression of CitH3, E) MPO levels, F-H) mRNA fold change of NETotic markersand I-M) Immunoblots and densitometric quantifications of MPO, PAD-4, NE and CitH3 in dHL-60 cells. The images were taken at 20X magnification. All the results are expressed as mean ± SEM of n=3. *p<0.05, **p<0.01 and ****p<0.0001 vs control, #p<0.05, ##p<0.01, ###p<0.001 and ####p<0.0001 vs PMA.

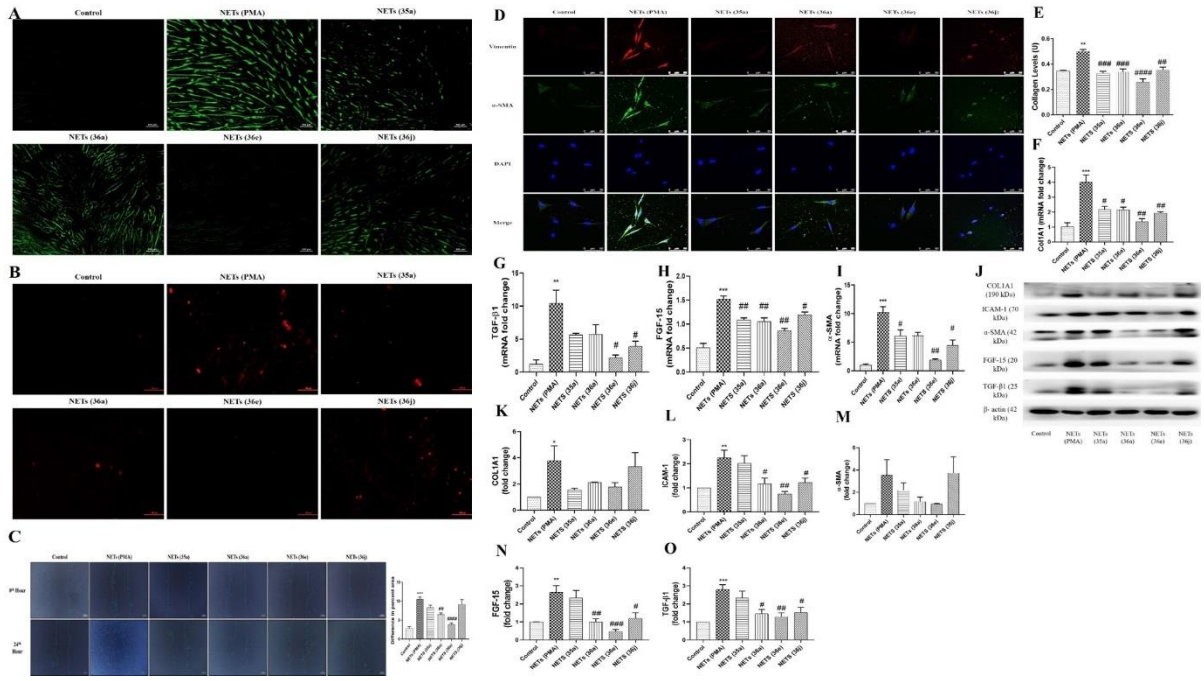

Figure 6: Effects of the NETs induced with PMA and treated with selected NCEs (35a, 36a, 36e and 36j) on A) Cellular ROS, B) Mitochondrial ROS, C) Cell migration(n=5), D-O) Fibrotic markers quantified through biochemical assay(n=3), WB(n=3) and RT-PCR(n=3). DCFDA and mitoSOX images were taken at 20X magnification, cell migration images at 10X magnification and confocal images at 63X magnification. All the results are expressed as

mean±SEM. *p<0.05, **p<0.01 and ***p<0.001 vs control, #p<0.05, ##p<0.01, ###p<0.001 and ####p<0.0001 vs NETs (PMA).

5.3 Evaluation of *in vivo* anti-fibrotic effects of the most potent PAD-4 inhibitor and study itsfibrosis resolving effects

5.3.1 Experimental Design

The animals were divided into seven groups after randomisation with 8 animals in each group. PF was induced with BLM at 1.5 U/kg on day 0 through oro-pharyngal instillation. 36e was administered as 3 mg/kg and 10 mg/kg through IP route and 30 mg/kg through oral route. One group received 5 mg/kg of CLA through IP route and the seventh treatment group received the PFD at 200 mg/kg dose through oral route. The treatment was continued for a period of 28 days. After the treatment, animals were euthanized, BALF, bone marrow and organ was isolated and subjected to molecular analysis.

5.3.2 Results

From the results obtained from *in vitro* analysis, we selected 36e molecule for detailed analysis of anti-fibrotic effects in BLM induced PF mice model. Induction of PF with BLM led to decrease in breathe frequency and minute volume and increased airway resistance, inspiration time and expiration time (Figure 7A). Treatment with 36e significantly normalised these parameters with the IP high dose and the oral dose showing higher treatment effects than other treatment options. This is also corroborated from increased body weight of the treatment groups and reduced lung weight/body weight ratio where treatment with 36e has resulted in significant improvement which can also be observed from pictorial representation of the representative lung images from specific groups (Figure 7B-D). Further, treatment with 36e resulted in mitigation of BLM induced abnormal BALF parameters such as higher total cell count, higher count of neutrophils and macrophages in BALF and higher levels of LDH, albumin and total protein in the BALF (Figure 7E). Upon isolation of neutrophils from bone marrow, it was observed that due to inflammation and fibrosis, the bone marrow of the diseased group had significantly higher production of neutrophils, which had higher NETotic potential. However, the bone marrow of treated animals showed decreased production of neutrophils with reduced NETotic potential (Figure 7F). Moreover, BLM induced fibrotic lungs showed higher levels of nitrite, MDA and lower levels of anti-oxidant GSH depicting higher oxidative stress. The increased oxidative stress is coupled with increased levels of pro-inflammatory cytokines like IL-6, IL-1β and TNF-α. Treatment with 36e reduced the levels of nitrite, MDA and increased the levels of anti-oxidant GSH (Figure 7G). Further, it also led to decreased levels of pro-inflammatory cytokines in lung tissues (Figure 7H). The histological analysis showed BLM induced fibrotic lungs showed typical features of fibrosis including honeycombing structure, degeneration of alveolar septa, decreased alveolar space and increased infiltration of cells inside the alveoli. This is accompanied by deposition of collagen in the lungs. Treatment with 36e reduced honeycombing structure with demarcation of alveolar septa and decreased infiltration of inflammatory cells and reduced deposition of collagen (Figure 7I). This is followed by evaluation of fibrotic markers in the lungs where the BLM induced fibrotic lungs showed increased level of fibrotic markers. It showed higher levels of hydroxyproline, increased mRNA and protein expression of COL1A1, fibronectin, vimentin, ICAM-1, α-SMA, SNAIL, SLUG and the pro-fibrotic cytokines TGF-β1. However, these expressions were effectively reduced upon treatment with PAD-4 inhibitor 36e. It significantly reduced the ECM proteins like COL1A1 and fibronectin, mesenchymal cell markers like α-SMA and vimentin,

fibrogenesis markers like ICAM-1 and hydroxyproline and transcription factors essential for EMT like SNAIL and SLUG (Figure 7J-R). We finally evaluated the effects of 36 PAD-4 inhibitors on PAD-4 levelsand other NETotic markers. It is evident from the studies that BLM induction led to significantly higher amount of circulating neutrophils and NETs in the alveoli as depicted through the sytox green and Ly6G staining analysis which is supported with increased mRNA and protein expression of PAD-4, NE, MPO and CitH3. 36e being a PAD-4 inhibitor reduced the levels of circulating neutrophils and NETs in the alveoli. It also led to significant inhibition in NETotic markers expressionlike NE, MPO and CitH3 with 36e IP high dose and oral dose showing significantly increased activity in almost all of the analysed parameters (Figure 7S-Y). Hence, it was confirmed that synthesised NCE 36e showed significant inhibition of inflammatory, fibrotic and NETotic markers in *in vitro* and *in vivo* models of NETosis and PF.

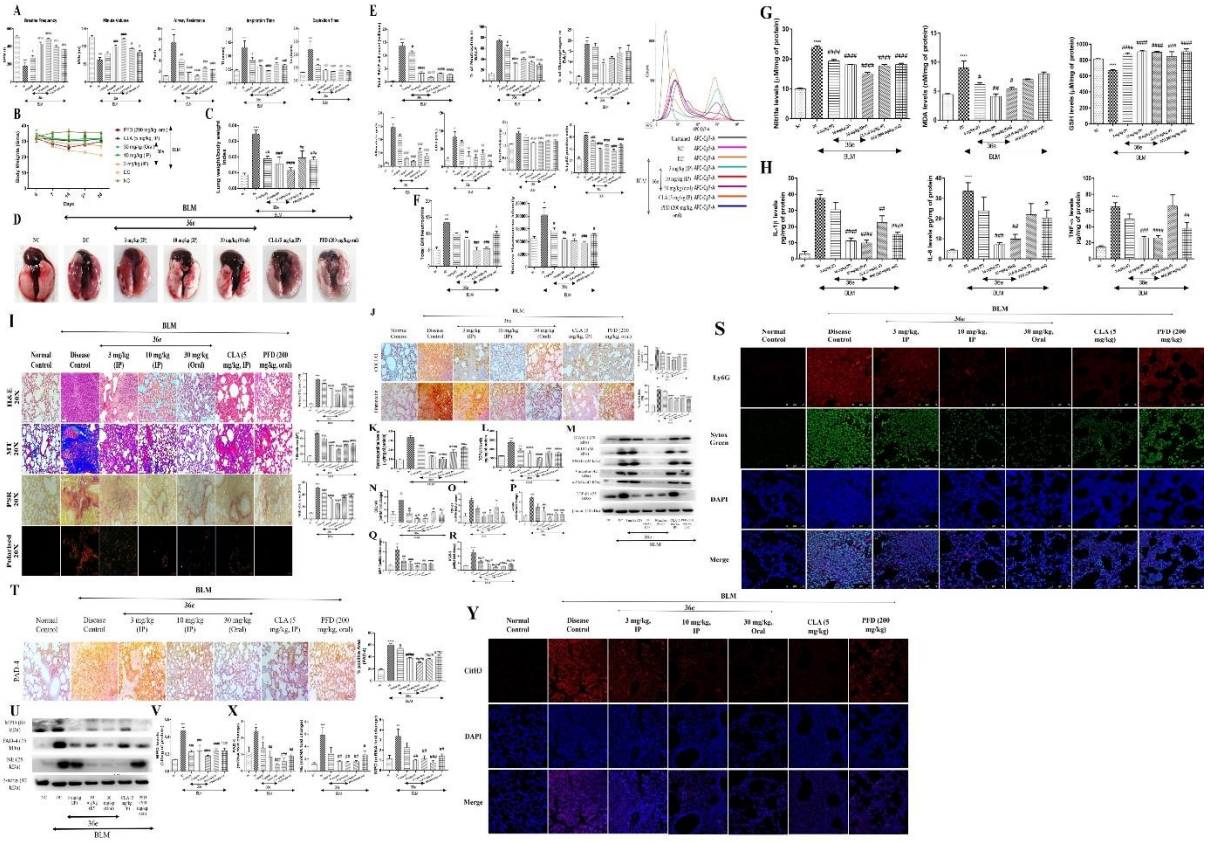

Figure 7: Effects of PAD-4 inhibitor on A) Lung functional parameters, B) Body weight of animals, C) Lung weight/body weight index, D) Lung morphology and appearance(n=8), E) BALF parameters(n=4), F) Neutrophilic parameters(n=4), G) Oxidative stress markers(n=8), H) Pro-inflammatory cytokines quantified through ELISA(n=8), I) Lung histology, collagen deposition and their quantification(n=10), J-R) Expression of fibrotic markers quantified through ELISA(n=8), biochemical assay(n=8), IHC(n=3), WB(n=3) and RT-PCR(n=4), S) Ly6G expression and NETs release, T-X) Expression of NETotic markers quantified through biochemical assay(n=8), IHC(n=3), WB(n=3) and RT-PCR(n=4) and Y) Expression of the NETotic marker CitH3. H&E, MT, PCR, polarised and IHC images were taken at 20X and confocal images at 40X magnification. All the results are expressed as mean±SEM. *p< 0.05, **p<0.01, ***p<0.001 and ****p<0.001 vs NC, #p<0.05, ##p<0.01, ###p<0.001 and ####p<0.0001 vs DC.

6. Discussion

Pulmonary fibrosis is one of the progressive lung disorder characterised by scarring of the lung tissue developed from an extended wound healing process. When the lungs sustain an injury, the local environment initiates a repair process involving the infiltration of immune cells such as neutrophils, macrophages, leukocytes, T cells, and B cells into the alveoli. These immune cells release a multitude of pro-inflammatory and pro-fibrotic cytokines, chemokines, and inflammatory mediators in an attempt to mend the damaged tissue. They stimulate fibroblasts to differentiate into myofibroblasts, which play a crucial role in the synthesis and secretion of collagen and other ECM components, thus kick-starting tissue remodelling. However, bizarre initiation and dysregulated termination of myofibroblast tend to cause a relentless accumulation of ECM, thus causing alveolar epithelium disintegration leading to organ dysfunction.

Our sytox green and DAPI staining studies confirmed CLA as a direct PAD-4 inhibitor, reducing NETs release and MPO levels. Immunocytochemistry revealed decreased PAD-4 expression with CLA treatment, reinforcing its anti-NETotic effects. CLA also controlled inflammatory markers like reactive oxygen and nitrogen species.

BLM instillation led to shrinkage of the alveolar space and thickening of the alveolar wall in addition to degradation of the alveolar septa. This in turn results in decreased breathing frequency, tidal volume and minute volume and increased airway resistance, inspiration time and expiration time. Treatment with CLA exerted protective effects which was attributed to normalising these lung function parameters. In accordance with this, there was development of fibrotic lesions inflammatory spots in the lungs which led to increase in lung weights. CLA further alleviated these features and the lungs were significantly normalised following CLA treatment which was reflected in the lung weights as well. Inflammatory cells migrate to the site of inflammation by disrupting the endothelial barrier. In the BLM induced PF, there was increase in total cell count, percentage of neutrophils and lymphocytes in the BALF that corroborated our pulmonary fibrosis research conducted in our lab (6,7,32). Supporting these findings are increase in total protein and albumin content in the BALF in BLM control group. These parameters were significantly reduced upon CLA treatment. Inflammation in the lungs triggered increased production and circulation of neutrophils in the whole blood which had greater than normal NETotic capacity. Out study testified the same where there was significant increase in total neutrophils in the whole blood with increased NETotic potential as depicted from sytox green dye binding assay. CLA treatment normalised these parameters as well.

Enhanced infiltration of inflammatory cells and oedema disrupt the normal architecture of the lungs upon BLM induction. It was significantly improved upon CLA treatment. Micro-injury to the lungs with BLM leads to persistent tissue injury initiating a cycle of repair and remodelling leading to deposition of ECM, increase in adhesive proteins and markers for EMT (58). The effect of CLA treatment on deposition of the collagen which is the primary component of the ECM was evaluated. Collagen specific staining techniques such as MT and PSR revealed a significant increase in collagen deposition in the BLM alone group whereas reduced collagen deposition was observed in the CLA treated lung sections indicating lesser degree of collagen deposition. Moreover, the expression of COL1A1 was also evaluated through immunohistochemistry and immunoblotting experiments. BLM treated mice affirmed higher COL1A1 expression which was dose-dependently lowered upon CLA treatment. Moreover, the expression of fibronectin which is an adhesive glycoprotein and has an important role to play in tissue repair and α-SMA which is a mesenchymal marker were greatly increased in the diseased tissue sections. Anti-fibrotic effects of CLA were also confirmed upon decreased expression of these proteins. Inflammation and fibrosis go hand in hand. Sustained

inflammation in the lung epithelium as a result of continuous and dysregulated stimulation by several factors contribute to the progress of PF. BLM induced lung tissue showed several fold increase in pro-inflammatory and pro-fibrotic cytokines such as TNF-α, IL-6, IL-1β and TGF-β as evidenced from ELISA studies. Treatment with CLA dampened these expressions thus validating anti-inflammatory and anti-fibrotic effects of CLA.

As mentioned above, migration of inflammatory cells into the alveolar spaces and BALF is an important feature of PF. Neutrophil migration is one of the critical step in inflammatory infiltration having paramount importance. Upon migration into the alveolar spaces, they carry out phagocytosis and NETosis and form the vicious cycle of inflammation. NE, MPO, CitH3 and PAD-4 are the decisive markers for NETosis. We evaluated their expressions in lung tissues through immunofluorescence, immunoblotting and RT-PCR experiments. Levels of MPO and expression of NE, CitH3 and PAD-4 had increased to several folds in the diseased lung. CLA dominantly decreased the levels of MPO and expressions of NE, CitH3 and PAD-4 in a dose-dependent manner.

We also evaluated the role of PAD-4 inhibitors on p53 and Del-1 expression in lung tissues. Owing to the fact that Del-1 is prominently expressed in the lungs endothelium, the normal lung showed a significant expression of Del-1 as evident from immunofluorescence, immunoblotting and RT-PCR experiments. Moreover, p53 was also expressed significantly in the normal lung tissue. However, the expression and positivity of Del-1 and p53 declined significantly to several fold in the diseased lung tissues. Interestingly, PAD-4 inhibitor CLA effectively normalised the expression of both p53 and Del-1 in both the dose groups with higher dose showing significant normalisation. The array of results obtained affirmed the fibrogenesis effects of PAD-4 and PAD-4 inhibitor can significantly result in anti-fibrotic effects. It also corroborates our hypothesis that expression of anti-inflammatory molecule Del-1 is decreased in a significant way in the diseases fibrotic lung tissues and treatment with PAD-4 inhibitor resulted in significantly normalised levels. Moreover, due to the fact that p53 expression also followed a similar pattern, it can be deduced that PAD-4 can have a significant role to play in co-repressing the expressions of Del-1 and p53.

After detailed analysis of molecular docking results, the focus shifted towards synthesizing selected molecules; where the primary aim was to synthesize indole-pyrazolopyrimidine derivatives. The synthesis of indole-pyrazolopyrimidine derivatives was carried as per the known procedures which included three key intermediates i.e. indole-pyrazole amines α,β-unsaturated carbonyls and benzylidenes We have synthesized 23 molecules of indole-pyrazolopyrimidine series.

Following synthesis the anti-NETotic and anti-fibrotic effects of the NCEs were carried out. They were first subjected to selective PAD-4 inhibition. All the 23 synthesised molecules were subjected to kit based PAD-4 enzyme inhibition which revealed the best IC50 of enzyme inhibition of the molecule 36e to be 5.64μM. Further, cytotoxicity and percentage of NETs inhibition of the NCEs were also evaluated. Based on the results 4 molecules namely 35a, 36a, 36e and 36j were selected for further studies. ROS are an important component of NETs. PMA induced NETs increased the levels of ROS and nitrite to several folds which was significantly inhibited by the NCEs. Extended assay on NETs release through flow cytometry and fluorescence imaging revealed strong reduction in NETs release reflected by decreased sytox green positivity in the treated dHL-60 cells. NE, MPO and CitH3 are the hall mark markers for NETosis. Although they are released along-with NETs. NE and MPO have controversial role in chromatin decondensation and have a significant role with PAD-4 in releasing NETs. Our NETs led to significant decrease in immunopositivity of CitH3 with higher reduction shown by 36e molecule. The NCEs also inhibited the MPO levels in the treated cells in comparison to

PMA stimulated cells. Moreover, PMA induction led to significant increased expression of mRNA of PAD-4, MPO, NE and MPO due to NETs induction. However, the mRNA expression of these markers were also reduced upon NCE treatment. These assays confirmed the anti-NETotic effects of the NCEs. We then stimulated the dHL-60 cells with PMA and treated them with NCEs followed by which we isolated the NETs from the stimulated and the treated cells. The untreated and treated NETs were exposed to fibroblasts to evaluate the effect of NETs inhibition on fibrotic parameters. Several reports are available showing higher induction of fibroblasts and their differentiation to myofibroblasts in in vitro fibroblasts. They have shown increased markers for myofibroblasts upon induction with untreated NETs. Upon isolating the NETs we exposed them to MRC-5 fibroblasts and evaluated the anti-fibrotic effects. However, we first evaluated the levels of ROS upon exposure to NETs in fibroblasts. The untreated NETs led to significant induction of ROS reflected by higher intensity of DCFDA fluorescence. The treated NETs had significant lower levels of ROS with higher reduction shown by the 36e treated NETs. Migration is an important features of fibroblasts. The fibroblasts tend to migrate the site of wound in order to repair it. In vitro wound scratch assay is an important tool to measure the migratory potential of the fibroblasts. The fibroblasts exposed to untreated NETs showed highest level of migration with very little space in the created wound. While, other treated NETs also led to migration, fibroblasts treated with 36e treated NETs showed significant decrease in cell migration depicting their potential. Further, we also evaluate the markers for fibrosis, myofibroblasts and mesenchymal cells including collagen, α-SMA, vimentin, FGF and TGF-β1. It was observed that the fibroblasts exposed to untreated NETs showed increased levels of collagen, α-SMA and vimentin. They also demonstrated increased mRNA expression of α-SMA, COL1A1, FGF and TGF-β1. The treated NETs had significant inhibition on protein expressions of collagen, α-SMA and vimentin and mRNA expressions of α-SMA, COL1A1, FGF and TGF-β1 with the 36e treated NETs showing higher inhibition. The selected NCEs had significant inhibition on NETs and fibrosis however, 36e was the NCE showing higher docking score, higher percentage of NETs inhibition and higher inhibition of PAD-4. Hence, the NCE 36e was the compound selected for in vivo anti-fibrotic effects in BLM induced PF in Swiss Albino mice.

The selected NCE was administered in three doses namely 3 mg/kg and 10 mg/kg through IP route and 30 mg/kg through oral route. The effects of 36e were compared with the standard PAD-4 inhibitor i.e. CLA and the FDA approved anti-fibrotic drug which is PFD.

Induction of fibrosis with BLM results in increased infiltration of inflammatory cells into the lung interstitium. Majorly neutrophils, macrophages and lymphocytes are the primary infiltrated cells and they initiate an inflammatory reaction. Increased inflammation leads to activation of fibroblasts and their differentiation into myofibroblasts, induction of EMT and the protein of ECM including collagen, vimentin and fibronectin are deposited in order to repair the injured and inflamed tissue. However, decreased termination and exaggeration of inflammatory and fibrosis reaction give rise to fibrotic tissue. BLM induction resulted in significant abnormality in the lung functional parameters such as breathe frequency, minute volume, airway resistance, inspiration time and expiration time. BLM led to significant decrease in breathe frequency and minute volume and significant increase in resistance of the airways, time of inspiration and time for expiration. The induction of fibrosis also leads to decrease in body weight and deposition of ECM leads to increase in lung weight. The pictorial representation effectively corroborated the fibrosis induction in the diseases lung by BLM. On the contrary, the treatment agents including 36e, CLA and PFD resisted the abnormality in lung functional tests. For instance, the breathe frequency, minute volume, airway resistance, inspiration time and expiration time were restored in the treated animals. The lung weight of the treated animals were significantly lowered than the fibrotic lung which is depicted by

decreased lung weight/body weight ratio and pictorial representation of the lungs with greater amelioration shown by 36e oral group depicting its superiority in providing anti-fibrotic effects. Measuring the BALF content is one of the important factor to evaluate the extent of respiratory diseases including ARDS, PF and COPD. Induction of fibrosis with BLM led to higher number of total circulated BALF cells with higher percentage of neutrophils and macrophages in the diseased lung than normal control. Total protein, albumin and LDH are the measure of infiltration and inflammation of the lungs. BALF led to higher levels of total protein, albumin and LDH in the BALF. However, the BALF of the treated animals showed significant reduction in total cells, protein levels, albumin levels and LDH levels in the BALF reflecting the anti-fibrotic and anti-inflammatory effects of the PAD-4 inhibitors. Moreover, we evaluated the percentage of neutrophils in BALF through flow cytometric analysis with Ly6G antibody. Ly6G is a surface antigen present on the neutrophils. The BALF from fibrotic animals showed higher percentage of Ly6G positive cells which was significantly reduced in the treated groups. Overall the 36e high dose and oral dose showed significant amelioration of the BALF parameters. Induction of inflammation in the live animals led to over production of neutrophils in the bone marrow which are very much prone to NETosis. We isolated the neutrophils from bone marrow and observed that the BLM group animals had significant higher levels of neutrophils content that significantly undergone NETosis upon PMA (500 nM) stimulation. However, there was significant decrease in the neutrophils from bone marrow of treated animals with decreased NETotic potential indicating reduction in overall inflammation by the PAD-4 inhibitors and PFD.

As mentioned earlier, BLM induction leads to significant infiltration of inflammatory cells and these cells infiltrate the alveolar spaces leaving very much less free alveolar space and degenerated alveolar septa. Moreover, induction of inflammation also leads to shrinkage of the available alveolar space which is reflected from H&E images of the lung sections and quantified with Ashcroft scoring. Moreover, we also evaluated the deposition of collagen in the lung tissues with staining with collagen specific dye including MT and PSR. Higher blue colour in MT and higher red colour in PSR were observed in the diseases tissue demonstrating higher deposition of collagen. However, the treated lung sections showed decreased shrinkage of the alveolar space, decreased infiltration, reduced oedematous tissue and decreased collagen deposition. All the treatment interventions showed amelioration of the pathological consequences induced by BLM with higher amelioration shown by 36e high dose and 36e oral group. This was followed by evaluating the levels of oxidative stress markers including nitrite, MDA and evaluating the levels of anti-oxidant GSH. The fibrotic lung tissues showed increased levels of nitrite and MDA and decreased GSH levels showing higher oxidative stress. The increase in oxidative stress was coupled with increased levels of pro-inflammatory cytokines including TNF-α, IL-6 and IL-1β. Treatment with the PAD-4 inhibitors led to decreased levels of nitrite, MDA and increased levels of GSH indicating reduction of oxidative stress. Moreover, they also reduced the levels of the pro-inflammatory cytokines to several folds with greater reduction shown by 36e oral dose treated animals. We then evaluated the markers for fibrosis including expression of proteins of the ECM, markers of mesenchymal cells, molecular markers for fibrogenesis and matrix remodelling. The fibrotic lung showed higher protein and mRNA levels of TGF-β1 which is the primary pro-fibrotic cytokine that induced fibroblast proliferation and differentiation. They also showed increased levels of Hydroxyproline that is a hydroxylatedproline moiety helping collagen stability and buildup. The increase in hydroxyproline amino acid is also corroborated with higher immunopositivity for COL1A1 protein in the fibrotic lung sections and higher mRNA expression of COL1A1 in the lung tissues. We also observed increased immunopositivity for fibronectin which is yet another protein of ECM. We further observed increased mRNA levels of α-SMA, ICAM-1 and

MMP-2 that are mesenchymal cell markers and marker for fibrogenesis and matrix remodelling. Treatment with the PAD-4 inhibitors including 36e and CLA and PFD showed decreased levels of hydroxyproline, decreased immunopositivity and mRNA expression of COL1A1, reduced mRNA and protein levels of TGF-β1 and reduced mRNA levels of α-SMA, ICAM-1 and MMP-2 reflecting its anti-fibrotic potential. Next, we estimated the inhibitory effects of NETosis by the novel PAD-4 inhibitor which was compared with the standard inhibitor CLA and anti-fibrotic drug PFD. Firstly, BLM resulted in higher immunopositivity of Ly6G and sytox green on lung sections indicating higher circulating neutrophils and NETs release. Moroever, BLM led to higher immunopositivity and mRNA expression of PAD-4 with higher protein and mRNA levels of MPO and NE. BLM induced fibrotic lung also showed higher immunopositivity of CitH3, yet another marker for NETosis. Treatment with 36e reduced Ly6G protein expression, sytox green intensity, protein and mRNA levels of PAD-4, MPO and NE. It also resulted in decreased levels of CitH3 in the treated lung sections. CLA being a standard NET inhibitor also significantly inhibited these NETotic markers, however, 36e had better outcome than CLA and PFD in inhibiting NETosis.

Thus, the in vitro and in vivo studies confirmed the anti-NETotic and anti-fibrotic effects of the NCEs with most prominent effects shown by 36e high dose and 36e oral dose. 36e effectively ameliorated fibrotic incidence in animals with significant anti-fibrotic and anti-NETotic effects.

7. Impact of the research in the advancement of knowledge or benefit to mankind

PF is a life-threatening disorder that has garnered significant importance following the outbreak of COVID-19. As mentioned several times in this document, PF results from a repetitive injury to the lungs that initiate an exaggerated immune response resulting in release of pro-inflammatory and pro-fibrotic cytokines which in turn lead to a dysregulated fibrotic response involving activation and differentiation of fibroblasts and myofibroblasts. The prolonged action of fibroblasts and myofibroblasts results in EMT and excessive deposition of ECM leading to lung fatality. COVID-19 was one such infection that resulted in a prolonged micro-injury to the lungs leading to exaggerated immune response. The patients infected with COVID-19 are highly susceptible to PF. Moreover, the worldwide incidence of PF is also alarming. The prevalence estimate of PF ranges from 0.33 to 2.51 per 10,000 persons in Europe to 2.40-2.98 per 10,000 persons in America (34). There are only two FDA approved drugs available in the market. The irregularity in the fibrotic matrix and complex network of ECM protein has limited the availability of anti-fibrotic medications. While, the mechanisms of the two drugs are distinct and majorly unknown, PFD is thought to inhibit fibroblast proliferation and TGF-β1 signalling and EMT. On the other hand, Nintedanib is a small molecule that inhibits the tyrosine kinases of several growth factor receptors such as fibroblast growth factor (FGF), vascular endothelial growth factor receptor (VEGFR), platelet derived growth factor receptor (PDGFR) thereby it inhibits TGF-β1 signalling and also inhibits expression of proteins of ECM such as fibronectin (FN) and collagen 1A1 (COL1A1). However, both the drugs are associated with similar side effects including gastrointestinal complications such as anorexia, nausea, abdominal pain, dyspepsia, and gastrointestinal reflux diseases (GERD). Moreover, PFD is associated with photosensitivity reaction and hepatic dysfunction and NTD is associated with thromboembolism, hypothyroidism. To increase the spectrum of anti-fibrotic drugs, there is a great need of novel anti-fibrotic drugs that can inhibit cells of innate immune system such as neutrophils and macrophages, adaptive immune systems such as lymphocytes and fibroblast proliferation, thus targeting the inflammatory stage and wound healing or repair stage of fibrosis may provide accumulated anti-fibrotic effects. Our NCE is targeting PF through a

holistic approach where it is inhibiting the inflammatory pathways and fibrotic pathways. Although, the selected molecule need a lot of optimisation, it is a head start for us to develop potent NETotic inhibitor and anti-fibrotic therapies.

8. References

1. Song S, Yu Y. Progression on citrullination of proteins in gastrointestinal cancers. Front Oncol. 2019;9(JAN):1–6.
2. Panda B, Momin A, Devabattula G, Shrilekha C, Sharma A, Godugu C. Peptidyl arginine deiminase-4 inhibitor ameliorates pulmonary fibrosis through positive regulation of developmental endothelial locus-1. Int Immunopharmacol [Internet]. 2024;140:112861. Available from: https://www.sciencedirect.com/science/article/pii/S1567576924013821
3. Chrysanthopoulou A, Mitroulis I, Apostolidou E, Arelaki S, Mikroulis D, Konstantinidis T, et al. Neutrophil extracellular traps promote differentiation and function of fibroblasts. J Pathol. 2014;233(3):294–307.
4. Annaldas S, Saifi MA, Khurana A, Godugu C. Nimbolide ameliorates unilateral ureteral obstruction-induced renal fibrosis by inhibition of TGF-β and EMT/Slug signalling. Mol Immunol. 2019;112:247–55.
5. Bansod S, Doijad N, Godugu C. Berberine attenuates severity of chronic pancreatitis and fibrosis via AMPK-mediated inhibition of TGF-β1/Smad signaling and M2 polarization. Toxicol Appl Pharmacol. 2020;403:115162.
6. Karkale S, Khurana A, Saifi MA, Godugu C, Talla V. Oropharyngeal administration of silica in Swiss mice: A robust and reproducible model of occupational pulmonary fibrosis. Pulm Pharmacol Ther. 2018;51:32–40.
7. Pulivendala G, Bale S, Godugu C. Honokiol: A polyphenol neolignan ameliorates pulmonary fibrosis by inhibiting TGF-β/Smad signaling, matrix proteins and IL-6/CD44/STAT3 axis both in vitro and in vivo. Toxicol Appl Pharmacol. 2020;391:114913.
8. Kim KK, Sheppard D, Chapman HA. TGF-β1 signaling and tissue fibrosis. Cold Spring Harb Perspect Biol. 2018;10(4):1–34.
9. Wilson MS, Wynn TA. Pulmonary fibrosis: pathogenesis, etiology and regulation. Mucosal Immunol. 2009;2(2):103–21.
10. Ali SA, Saifi MA, Godugu C, Talla V. Silibinin alleviates silica-induced pulmonary fibrosis: Potential role in modulating inflammation and epithelial-mesenchymal transition. Phyther Res. 2021;35(9):5290–304.
11. Sravani S, Saifi MA, Godugu C. Riociguat ameliorates kidney injury and fibrosis in an animal model. Biochem Biophys Res Commun. 2020;530(4):706–12.
12. Kim D-Y, Lee S-H, Fu Y, Jing F, Kim W-Y, Hong S-B, et al. Del-1, an endogenous inhibitor of TGF-β activation, attenuates fibrosis. Front Immunol. 2020;11:68.
13. Hanayama R, Tanaka M, Miwa K, Nagata S. Expression of Developmental Endothelial Locus-1 in a Subset of Macrophages for Engulfment of Apoptotic Cells. J Immunol. 2004;172(6):3876–82.

14. Kang Y-Y, Kim D-Y, Lee S-H, Choi EY. Deficiency of developmental endothelial locus-1 (Del-1) aggravates bleomycin-induced pulmonary fibrosis in mice. Biochem Biophys Res Commun. 2014;445(2):369–74.

15. Kourtzelis I, Li X, Mitroulis I, Grosser D, Kajikawa T, Wang B, et al. DEL-1 promotes macrophage efferocytosis and clearance of inflammation. Nat Immunol [Internet]. 2019;20(1):40–9. Available from: http://dx.doi.org/10.1038/s41590-018-0249-1

16. Li P, Yao H, Zhang Z, Li M, Luo Y, Thompson PR, et al. Regulation of p53 target gene expression by peptidylarginine deiminase 4. Mol Cell Biol. 2008;28(15):4745–58.

17. Kim H, Lee SH, Lee MN, Oh GT, Choi KC, Choi EY. P53 regulates the transcription of the anti-inflammatory molecule developmental endothelial locus-1 (Del-1). Oncotarget. 2013;4(11):1976–85.

18. Lewallen DM, Bicker KL, Madoux F, Chase P, Anguish L, Coonrod S, et al. A FluoPol-ABPP PAD2 high-throughput screen identifies the first calcium site inhibitor targeting the PADs. ACS Chem Biol. 2014;9(4):913–21.

19. Dreyton CJ, Anderson ED, Subramanian V, Boger DL, Thompson PR. Insights into the mechanism of streptonigrin-induced protein arginine deiminase inactivation. Bioorg Med Chem. 2014;22(4):1362–9.

20. Knuckley B, Jones JE, Bachovchin DA, Slack J, Causey CP, Brown SJ, et al. A fluopol-ABPP HTS assay to identify PAD inhibitors. Chem Commun. 2010;46(38):7175–7.

21. Luo Y, Knuckley B, Lee Y-H, Stallcup MR, Thompson PR. A fluoroacetamidine-based inactivator of protein arginine deiminase 4: design, synthesis, and in vitro and in vivo evaluation. J Am Chem Soc. 2006;128(4):1092–3.

22. Luo Y, Knuckley B, Bhatia M, Pellechia PJ, Thompson PR. Activity-based protein profiling reagents for protein arginine deiminase 4 (PAD4): synthesis and in vitro evaluation of a fluorescently labeled probe. J Am Chem Soc. 2006;128(45):14468–9.

23. Luo Y, Arita K, Bhatia M, Knuckley B, Lee Y-H, Stallcup MR, et al. Inhibitors and inactivators of protein arginine deiminase 4: functional and structural characterization. Biochemistry. 2006;45(39):11727–36.

24. Bicker KL, Anguish L, Chumanevich AA, Cameron MD, Cui X, Witalison E, et al. D-amino acid-based protein arginine deiminase inhibitors: Synthesis, pharmacokinetics, and in cellulo efficacy. ACS Med Chem Lett. 2012;3(12):1081–5.

25. Causey CP, Jones JE, Slack JL, Kamei D, Jones Jr LE, Subramanian V, et al. The development of N-α-(2-carboxyl) benzoyl-N 5-(2-fluoro-1-iminoethyl)-l-ornithine amide (o-F-amidine) and N-α-(2-carboxyl) benzoyl-N 5-(2-chloro-1-iminoethyl)-l-ornithine amide (o-Cl-amidine) as second generation protein arginine deiminase (PAD) inhibit. J Med Chem. 2011;54(19):6919–35.

26. Jones JE, Slack JL, Fang P, Zhang X, Subramanian V, Causey CP, et al. Synthesis and screening of a haloacetamidine containing library to identify PAD4 selective inhibitors. ACS Chem Biol. 2012;7(1):160–5.

27. Knight JS, Subramanian V, O'Dell AA, Yalavarthi S, Zhao W, Smith CK, et al. Peptidylarginine deiminase inhibition disrupts NET formation and protects against kidney, skin and vascular disease in lupus-prone MRL/lpr mice. Ann Rheum Dis. 2015;74(12):2199–206.

28. Muth A, Subramanian V, Beaumont E, Nagar M, Kerry P, McEwan P, et al. Development of a selective inhibitor of protein arginine deiminase 2. J Med Chem. 2017;60(7):3198–211.

29. Najmeh S, Cools-Lartigue J, Giannias B, Spicer J, Ferri LE. Simplified human neutrophil extracellular traps (NETs) isolation and handling. JoVE (Journal Vis Exp. 2015;(98):e52687.

30. Pooladanda V, Thatikonda S, Bale S, Pattnaik B, Sigalapalli DK, Bathini NB, et al. Nimbolide protects against endotoxin-induced acute respiratory distress syndrome by inhibiting TNF-α mediated NF-κB and HDAC-3 nuclear translocation. Cell Death Dis. 2019;10(2):1–17.

31. Pooladanda V, Thatikonda S, Muvvala SP, Devabattula G, Godugu C. BRD4 targeting nanotherapy prevents lipopolysaccharide induced acute respiratory distress syndrome. Int J Pharm. 2021;601:120536.

32. Boyapally R, Pulivendala G, Bale S, Godugu C. Niclosamide alleviates pulmonary fibrosis in vitro and in vivo by attenuation of epithelial-to-mesenchymal transition, matrix proteins & Wnt/β-catenin signaling: A drug repurposing study. Life Sci. 2019;220:8–20.

33. Bansod S, Khurana A, Godugu C. Cerulein-induced chronic pancreatitis in Swiss albino mice: An improved short-term model for pharmacological screening. J Pharmacol Toxicol Methods. 2019;96:46–55.

34. Pergolizzi Jr J V, LeQuang JA, Varrassi M, Breve F, Magnusson P, Varrassi G. What Do We Need to Know About Rising Rates of Idiopathic Pulmonary Fibrosis? A Narrative Review and Update. Adv Ther. 2023;40(4):1334–46.